

Metabolic Profiling Uncovers a Phenotypic Signature of Small for Gestational Age in Early Pregnancy

Richard P Horgan,[†] David I. Broadhurst,^{†,‡} Sarah K. Walsh,[†] Warwick B. Dunn,^{§,||} Marie Brown,^{||} Claire T. Roberts,^{⊥,‡} Robyn A. North,^{‡,¶} Lesley M. McCowan,^{‡,▲} Douglas B. Kell,[§] Philip N. Baker,^{‡,‡} and Louise C. Kenny^{*,†,‡}

[†]The Anu Research Centre, Department of Obstetrics and Gynaecology, University College Cork, Cork University Maternity Hospital, Cork, Ireland

[§]The Manchester Centre for Integrative Systems Biology and the School of Chemistry, Manchester Interdisciplinary Biocentre, The University of Manchester, Manchester, M1 7DN, United Kingdom

^{||}Centre for Advanced Discovery and Experimental Therapeutics and School of Biomedicine, Manchester Biomedical Research Centre, University of Manchester, Manchester, M13 9WL, United Kingdom

[⊥]Research Centre for Reproductive Health, Robinson Institute, School of Paediatrics and Reproductive Health, University of Adelaide, Australia 5005

[¶]Division of Reproduction and Endocrinology, King's College London, United Kingdom

[▲]Department of Obstetrics and Gynaecology, University of Auckland, Auckland, New Zealand

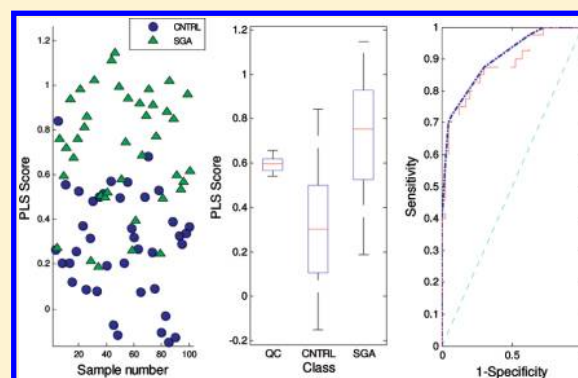
[‡]Faculty of Medicine & Dentistry, University of Alberta, Edmonton, AB T6G 2R7 Canada

^{*}The SCOPE Consortium

S Supporting Information

ABSTRACT: Being born small for gestational age (SGA) confers increased risks of perinatal morbidity and mortality and increases the risk of cardiovascular complications and diabetes in later life. Accumulating evidence suggests that the etiology of SGA is usually associated with poor placental vascular development in early pregnancy. We examined metabolomic profiles using ultra performance liquid chromatography–mass spectrometry (UPLC–MS) in three independent studies: (a) venous cord plasma from normal and SGA babies, (b) plasma from a rat model of placental insufficiency and controls, and (c) early pregnancy peripheral plasma samples from women who subsequently delivered a SGA baby and controls. Multivariate analysis by cross-validated Partial Least Squares Discriminant Analysis (PLS-DA) of all 3 studies showed a comprehensive and similar disruption of plasma metabolism. A multivariate predictive model combining 19 metabolites produced by a Genetic Algorithm-based search program gave an Odds Ratio for developing SGA of 44, with an area under the Receiver Operator Characteristic curve of 0.9. Sphingolipids, phospholipids, carnitines, and fatty acids were among this panel of metabolites. The finding of a consistent discriminatory metabolite signature in early pregnancy plasma preceding the onset of SGA offers insight into disease pathogenesis and offers the promise of a robust presymptomatic screening test.

KEYWORDS: small for gestational age, fetal growth restriction, placental insufficiency, RUPP – reduced uterine perfusion pressure, metabolomics, metabolic profiling, ultra performance liquid chromatography–mass spectrometry, pregnancy, plasma



■ INTRODUCTION

Being born small for gestational age (SGA) affects 3–10% of nulliparous pregnancies and confers significantly increased risks of perinatal morbidity and mortality. SGA is associated with at least 25% of all stillbirths,¹ and recent evidence suggests this figure is possibly as high as 50%.² There is an increased risk of learning difficulties and cerebral palsy in survivors,^{3,4} and recent studies have suggested that SGA affects both the long-term development and homeostasis of the endocrine system in later

life, inducing complications such as hypertension, coronary heart disease, hypercholesterolemia, and diabetes.^{5–8}

SGA is most commonly defined as less than the 10th centile of birthweight by a specific gestational age.⁹ More recently customized birthweight centiles (correcting for maternal height, maternal weight at booking, ethnic origin, parity, sex of fetus,

Received: March 30, 2011

Published: June 14, 2011

and gestational age) have been proposed as a more effective way of identifying SGA pregnancies associated with morbidity and mortality.^{10,11} However, even when defined using customized centiles, it is estimated that one-third of all fetuses below the 10th customized birthweight centile are constitutionally small and are thus misdiagnosed as being at high-risk of adverse outcome.¹¹ Because accurate diagnosis in the vast majority of cases may only be made with certainty after delivery, a significant number of fetuses that are healthy but SGA may be subjected to high-risk protocols and, potentially, iatrogenic prematurity. The clinician's challenge is not only to identify SGA fetuses whose health is endangered in utero and to monitor and intervene appropriately but also to identify constitutionally small but healthy fetuses and avoid iatrogenic harm to them or their mothers.

Presently, there is no accurate way of antenatally identifying nulliparous women who will subsequently deliver an SGA baby. Thus, the condition remains undiagnosed before birth in 40–80% of cases, contributing to the high rate of stillbirth.^{12–14} Several biomarkers for SGA have been proposed, including growth factors,^{15,16} placental hormones,^{17–19} and angiogenic factors;^{20–22} however, none (nor any combination) have shown satisfactory specificity and sensitivity to be clinically useful.

The majority of SGA infants at risk of adverse outcome are thought to be pathologically small secondary to fetal growth restriction (FGR); defined as a condition where a fetus is unable to achieve its genetically determined potential size.²³ In spite of the many known risk factors associated with SGA,²⁴ the underlying disease pathology of FGR is complex and not well understood. Accumulating evidence suggests that disease manifestation is due to poor placental vascular development in early pregnancy such that the fetus does not receive sufficient nutrients and oxygen needed for optimal growth and development throughout pregnancy.^{25–28} It has been postulated that trophoblast dysregulation at a subcellular level and loss of functional mass of villous trophoblast via cell death pathways are key contributors to the suboptimal placental perfusion that yields growth restriction.²⁹ In support of this, placentae from women who deliver SGA infants may have macroscopic evidence of infarction and microscopic changes including increased formation of syncytial knots, reduced cytotrophoblast proliferation, and increased apoptosis when compared with placentae from pregnancies resulting in normal birthweight infants.^{30,31}

We therefore hypothesized that poor placental perfusion will result in altered levels of biochemical factors in both maternal and fetal blood throughout pregnancy when compared to normal healthy pregnancy, reflecting the poor transfer of nutrients and oxygen to and waste products from the fetus. As trophoblast differentiation and invasion begin in early pregnancy, we also hypothesized that subsequent suboptimal placental perfusion will also commence early in pregnancy. Detecting a biochemical phenotypic signature early in pregnancy, prior to clinical diagnosis, could yield an effective presymptomatic screening tool for SGA.

Metabolic profiling^{32–41} is a powerful systems biology strategy for investigating the low molecular weight biochemicals (metabolites) present in the metabolome of a cell, tissue, or organism.^{42–48} Its position as the final downstream product of gene expression enables the provision of a high resolution multifactorial phenotypic signature of disease etiology, manifestation, or pathophysiology.^{49–56}

Metabolomic technology can be used to analyze many different types of biofluid. Human blood is a complex sample type that generates thousands of metabolites⁵⁷ and reflects the metabolism

of multiple tissue and cell types in the mammalian body. We have demonstrated that this technology produces reproducible, robust, and valid results in metabolic profiling studies when using blood as an analyte.^{58,59} We and others have previously reported results of a metabolomic screen on plasma from women with established pre-eclampsia.^{49,60–62} We therefore sought to take a similar metabolomic approach for characterizing the metabolic phenotype of SGA in plasma.

The investigation presented here consisted of three consecutive but independent studies. First, the aim was to characterize the metabolic signature of SGA at a time-point as close as possible to that of clinical diagnosis such that a biochemical time-of-disease signature could be defined. This was achieved by analyzing plasma from the umbilical cord that drains the placental vasculature taken immediately after delivery. By sampling venous umbilical cord plasma, rather than maternal plasma, we were also able to determine a biochemical signature solely associated with fetal-placental interaction and not obscured by the metabolome by particular characteristics of the maternal circulatory system and its interaction with other organ systems.

Second, the time-of-disease metabolite biomarker signature was compared to the metabolic profile of an animal model of placental insufficiency, the reduced uterine perfusion pressure (RUPP) rat, where the phenotype of the pups and placentas at birth is comparable to severe growth restriction.^{63,64} Several animal models of abnormal fetal growth exist;^{65,66} however, most involve either stressing the animal (e.g., hypoxia) or imposing strict dietary regimes. The changes in metabolism due to genotype, diet and/or environment are difficult to differentiate from potential biomarkers due to placental insufficiency. The RUPP model, which involves a mechanical intervention to restrict blood flow to the placenta, removes these concerns as any resulting changes in metabolism is more likely to reflect placental etiology. By comparing the cord plasma metabolome to that of the RUPP model, we were able to assess to what degree the cord plasma biomarker signature reflected the phenotype of a highly constrained model of placental insufficiency.

Third, the cord plasma biomarker signature was compared to that from peripheral blood samples collected at 15 ± 1 weeks' gestation from women who subsequently delivered a SGA baby and matched controls. A nested case-control experiment was performed using a subset of women who were participants in the multinational Screening for Pregnancy End Points (SCOPE) study (www.scopestudy.net), a prospective cohort study of healthy nulliparous women.

Finally, comparable metabolite data from both the venous cord blood study and the week-15 study were mined to find a simple yet robust, metabolite rule that effectively predicts SGA in early pregnancy. The components of this simple metabolite signature were compared across all three studies.

■ MATERIALS AND METHODS

Participants and Specimens

(a). **Venous Cord Plasma.** Venous cord blood was obtained, within 20 min of delivery with written maternal consent in compliance with the Central Manchester Research Ethics Committee approval. Blood was collected from women with uncomplicated, term pregnancies resulting in delivery of a healthy singleton fetus ($n = 6$) and from women with suspected SGA, which was subsequently confirmed after delivery based on individualized birthweight centiles ($n = 8$)¹⁰ (www.gestation.net).

Pregnancies complicated by any other maternal or fetal factor, including pre-eclampsia, gestational hypertension, diabetes mellitus, and congenital anomalies were excluded. No dietary constraints were imposed on the participating women.

Plasma samples were collected into BD EDTA-Vacutainer tubes, placed on ice and centrifuged at $2400 \times g$ at 4°C for 10 min according to a standardized protocol. Plasma was stored in aliquots at -80°C . The collection and storage conditions were identical for cases and controls.

(b). RUPP Model. Pregnant Sprague–Dawley rats (12 weeks; supplied and maintained by the Biological Services Unit, University College Cork) were housed in the Biological Services Unit at University College Cork. Animals were maintained at a temperature of $21 \pm 2^\circ\text{C}$, with a 12-h light/dark cycle and with free access to food and tap water. All procedures were performed in accordance with national guidelines and the European Community Directive 86/609/EC and approved by the University College Cork Local Animal Experimentation Ethics Committee.

On day 14 of a 21 day pregnancy, animals destined for the RUPP experimental group were anesthetized with isoflurane (2–5% inhalation), and the abdominal cavity was opened via a midline incision to expose the lower abdominal aorta. A silver clip (0.203 mm ID) was placed around the aorta (above the iliac bifurcation) to reduce uterine perfusion pressure by approximately 40%.⁶⁷ Because compensation of blood flow to the placenta occurs via an adaptive response of the uterine arteries,⁶⁸ silver clips (0.10 mm ID) were also placed on the main uterine branches of both right and left uterine arteries. A series of experiments was also carried out in sham-operated animals (i.e., subjected to the same surgical procedure with the exception that the vessels were not partially occluded). On day 19 of pregnancy, all animals were anesthetized with isoflurane and blood was collected via the abdominal aorta into precooled heparinised vacutainers. All pups and placentas were removed, weighed, and litter size noted. Any animals in which the clipping procedure had resulted in total reabsorption of fetuses were excluded from the study. Blood collected into precooled heparinised vacutainers was centrifuged at $2400 \times g$ for 10 min at 4°C ; the plasma was then removed and stored in $250 \mu\text{L}$ aliquots at -80°C . Plasma for a total of 23 animals was collected for metabolomic analysis: 7 normal pregnant, 8 sham operated, and 8 RUPP.

(c). Week-15 Peripheral Plasma. All women were participants in the multinational SCOPE study. These samples are extremely well curated, accompanied by comprehensive meta-data, and are proportionally population matched to avoid potential sources of bias.⁶⁹ The SCOPE study is a prospective, cohort study with the main aim of developing accurate screening methods for later pregnancy complications, including SGA (ACTRN12607000551493). Full ethical approval has been obtained, and all patients gave written informed consent. Healthy nulliparous women with a singleton pregnancy were recruited between 14 and 16 weeks' gestation and tracked throughout pregnancy. No dietary constraints were imposed on the participating women throughout this study.

We performed a case control study within the initial 596 recruits from Adelaide, Australia, of whom pregnancy outcome was known in 595 (99.8%). Seventy-three (12.2%) women went on to deliver SGA babies and 267 (44.8%) had uncomplicated pregnancies. The remainder had other pregnancy complications. Forty women who developed SGA were matched for age, ethnicity, and BMI to 40 controls who had uncomplicated pregnancies.

Women with coexistent pre-eclampsia were excluded from the study.

Venipuncture was performed at 15 ± 1 weeks' gestation, and plasma samples were collected into BD EDTA-Vacutainer tubes, placed on ice, and centrifuged at $2400 \times g$ at 4°C according to a standardized protocol. Plasma was stored in aliquots at -80°C . The collection and storage conditions were identical for cases and controls, with the time between collection and storage being 2.07 (SD 0.90) and 2.02 (SD 0.96) hours, respectively, $P = 0.78$.

Reagents, Sample Preparation, and Mass Spectral Analysis

All chemicals and reagents used were of Analytical Reagent or HPLC grade and purchased from Sigma-Aldrich (Poole, UK) or ThermoFisher Scientific (Loughborough, U.K.). Plasma samples were allowed to thaw on ice for 3 h, vortex mixed to provide a homogeneous sample and deproteinised. To $100 \mu\text{L}$ of plasma was added $300 \mu\text{L}$ of methanol (HPLC grade) followed by vortex mixing (15 s, full speed) and centrifugation (15 min, $11\,337 \times g$). Two-hundred seventy microliter aliquots of the supernatant were transferred to a 2 mL tube and lyophilized (HETO VR MAXI vacuum centrifuge attached to a Thermo Svart RVT 4104 refrigerated vapor trap; Thermo Life Sciences, Basingstoke, U.K.). Quality Control (QC) samples were obtained by pooling $50 \mu\text{L}$ aliquots from each plasma sample prepared. This was defined as the pooled QC sample and $100 \mu\text{L}$ aliquots were deproteinised as described above.

Deproteinised samples were prepared for UPLC-MS analysis by reconstitution in $90 \mu\text{L}$ HPLC grade water followed by vortex mixing (15 s), centrifugation ($11\,337 \times g$, 15 min) and transfer to vials. Samples were analyzed by an Acquity UPLC (Waters Corp. Milford, MA) coupled to a hybrid LTQ-Orbitrap mass spectrometry system (Thermo Fisher Scientific, Bremen, Germany) operating in electrospray ionization mode as previously described.^{59,70} Samples were analyzed in batches of up to 120 samples, with an instrument maintenance step at the end of each batch involving mass spectrometer ion source and liquid chromatography column cleaning. For each analytical batch, a number of pooled QC samples were included to provide quality assurance. The first 10 injections were pooled QC samples (to equilibrate the analytical system) and then every fifth injection was a pooled QC sample. For each of the analytical experiments (venous cord plasma/RUPP/week-15), sample preparation order was randomized from sample picking and rerandomized before sample analysis to ensure no systematic biases (e.g., analysis order correlates with sample preparation order). The samples were also blinded to the analytical scientists to avoid any subjective bias. Each study was performed several months apart, such that all the studies could be considered independent both in terms of sample source and chemical analysis. Raw profile data were deconvolved into a peak table using XCMS software.⁷¹ Data were then subjected to strict Quality Assurance procedures so that statistical analysis was only performed on reproducible data. Full details of all methods pertaining to sample preparation, UPLC-MS analysis, and quality assurance are described in the attached supplementary methodology file (Supporting Information).

For the venous cord bloods study alone, three replicate plasma samples were analyzed per subject. These replicate samples were collected at the same sampling time-point, but subsequently included in the randomization of sample picking, preparation and injection order protocols. This oversampling design was implemented to allow validation of the overall analytical procedure, such that the within patient variability could be compared to the between class discrimination in subsequent statistical analysis. In this way the Quality Assurance procedure was also validated.

Statistical Analysis

Comparisons of clinical data between cases and controls were performed using the Student's *t* test, Mann–Whitney test, Chi square test or Fisher's Exact test, as appropriate (SAS system 9.1).

For each metabolite peak reproducibly detected in a given study, the null hypothesis that the means of the case and control sample populations were equal was tested using either the Mann–Whitney test or Student's *t* test, depending on data normality (assessed using the Lilliefors test). The critical *p*-value for significance was set to 0.05. Avoiding false positives by correcting for multiple comparisons was performed using False Discovery Rate (FDR)⁷² analysis and FDRs are quoted where appropriate. Comparisons across experiments were not corrected as this process of validation is deemed sufficient to remove any false positives. In addition, a Receiver–Operator Characteristic (ROC) curve was calculated to assess each peak's effectiveness as a univariate discriminatory biomarker. The area under the ROC curve (AUC) provides a good estimate of biomarker utility (an AUC = 1 demonstrates perfect biomarker separation; AUC = 0.5 demonstrates no utility at all).

Multivariate profile-wide predictive models were constructed using Partial Least Squares Discriminant Analysis (PLS-DA).^{73–75} For each model, all of the reproducible peaks for a given study were included, unless expressly stated. The number of latent variables in each model was selected using stratified 5-fold cross validation,⁷³ and associated R^2 and Q^2 statistics calculated. Here, R^2 , the squared correlation coefficient between the dependent variable and the PLS-DA prediction, measures “goodness-of-fit” (a value between zero and one, where one is a perfect correlation). Q^2 provides a measure of “goodness-of-prediction” and is the averaged correlation coefficient between the dependent variable and the PLS-DA predictions for the 5-fold out data sets generated during the cross-validation process.

Further validation was performed to check the robustness of the final PLS-DA model by comparing its Q^2 value to a reference distribution of all possible models using permutation testing ($N = 1000$) following the standard protocol for metabolomic studies.⁷⁶ Here a reference Q^2 distribution is obtained by calculating all possible PLS-DA models under random reassignment of the case/control labels for each measured metabolic profile. If the correctly labeled model's Q^2 value is close to the center of the reference distribution then the model performs no better than a randomly assigned model and is therefore invalid. For all PLS-DA models described here the associated reference distribution plots are provided, from which an estimate of the probability of the candidate model randomly occurring can be estimated. In addition, where appropriate, a receiver operating characteristic (ROC) curve was determined so that an accurate assessment of discriminatory ability could be made.

Finally, we searched for an “optimal” multivariate discriminatory model drawn from the named metabolites observed in both the venous cord plasma and week-15 studies. A Genetic Algorithm-based search program was used to obtain the subset of metabolites which produced an effective predictive rule for the onset of SGA. This search method has been shown to be very successful in previous studies.^{33,77–81} In this algorithm, a set of candidate solutions evolve over time toward an optimal state. The evolution is pushed by computational techniques inspired by evolutionary biology. In our algorithm, each candidate solution (subset of metabolites) is assessed by building two independent Linear Discriminant Analysis models, one modeling the venous cord plasma data, and the other modeling the week-15

data. A candidate's fitness is proportional to the sum of the root-mean-square error of prediction (RMSEP) of these two models. Once the optimal subset of metabolites was found, its predictive ability was assessed using PLS-DA. Assessment was performed independently for the venous cord plasma and week-15 data. In addition the final “rule” was tested using the RUPP model data to see if there was a consistent minimal signature across all three studies.

All peak data were Pareto scaled before multivariate analysis.⁸² All statistical analyses were carried out using the Matlab scripting language (<http://www.mathworks.com/>). All univariate algorithms were implemented such that any missing values are ignored. All multivariate algorithms were implemented such that missing values were imputed using the nearest-neighbor method.⁸³

Where appropriate, for the PLS-DA prediction scores, the optimal unbiased discriminatory decision boundary was estimated using the optimal Youden's index method⁸⁴ and then the associated discriminatory odds ratios with 95% confidence intervals (OR 95%CI) calculated.^{84,85}

Metabolite Identification

For identification of UPLC–MS peaks, the accurate mass for each peak was searched against The Manchester Metabolomics Database⁷¹ constructed with information from metabolic reconstructions,⁸⁶ both HMDB (<http://www.hmdb.ca/>) and Lipidmaps (<http://www.lipidmaps.org/>). The workflows applied are freely available.⁸⁷ A metabolite name(s) was reported when a match with a mass difference between observed and theoretical mass was less than 3 ppm. Using UPLC–MS, metabolites are often detected multiple times due to chemical adduction, dimerization, multiple-charging, isotope peaks and fragmentation. After removal of duplicate identifications, a list of unique metabolites was compiled. Definitive identifications were reported only for metabolites with retention time errors <10 s and an accurate mass match <5 ppm. Once identified, the metabolites were grouped into metabolite classes using the HMDB “Class” hierarchy (<http://www.hmdb.ca/>).

RESULTS

Venous Cord Plasma

Maternal characteristics and pregnancy outcomes of the cases and controls are described in Table 1. Age, BMI, parity, smoking and baby sex were carefully matched across cases and controls. All SGA babies had an individualized birthweight centile <10th centile.

Ultra performance liquid chromatography–mass spectrometry (UPLC–MS) analysis reproducibly detected a total of 2011 metabolite features. A cross-validated Partial Least Squares Discriminant Analysis (PLS-DA) model was built using two latent factors. The resulting scores plot (Figure 1) demonstrated clear differences between the SGA and control profiles with an $R^2 = 0.88$, $Q^2 = 0.81$. Permutation testing showed that the probability of a model of this quality randomly occurring was less than 0.001 (Supplementary Figure S1, Supporting Information). Figure 1 clearly shows that the analytical replicates (numbered) produce highly repeatable PLS scores.

Univariate hypothesis testing was performed across the 2011 detected metabolites. Prior to statistical analysis, the three analytical replicates were averaged, to avoid biased reduction of the significance values. With a critical *p*-value of 0.05, 744 metabolite features (37% of those detected) were found to have significant difference between SGA and control, with a false

discovery rate (FDR) of 6%, of which 96 were putatively identified as “unique” endogenous metabolites.

RUPP Model

RUPP pups were associated with restricted fetal growth, with respect to pup weight, when compared with normal pregnant (2.2 ± 0.1 versus 3.2 ± 0.1 g; $P < 0.001$) and sham-operated (2.2 ± 0.1 versus 3.2 ± 0.1 g; $P < 0.001$) pups (data not shown). Furthermore, placental weights from RUPP rats were also significantly reduced compared with both normal pregnant

Table 1. Maternal Characteristics and Pregnancy Outcomes of the SGA and Control Babies from Which the Venous Cord Plasma Samples Were Taken

maternal characteristics	control $n = 6$	SGA $n = 8$	p -value
Age (years)	24.5 (20.8–31.2)	30 (26.3–32.5)	0.33
Nulliparous	4	5	1.00
BMI kg/m^2	25.0 (22.0–27.1)	24.8 (21.8–25.5)	0.82
Current smoker	1	2	1.00
Sex (male)	4	4	0.63
Mode of Delivery			
- vaginal	4	2	0.28
- C/S	2	6	
Gestation at delivery (weeks)	38.5 (38.2–38.7)	39.0 (38.2–40.0)	0.15
Ethnicity			
- caucasian	4	3	0.59
- other	2	5	
Birthweight (g)	3040 (2945–3240)	2735 (2419–2813)	0.05
Customized birthweight centile	29 (19–58)	3 (2–5)	0.04

Values are median (interquartile range) or number. BMI = body mass index; C/S = caesarean section.

(0.33 ± 0.01 versus 0.43 ± 0.01 g; $P < 0.001$) and sham operated (0.33 ± 0.01 versus 0.42 ± 0.02 g; $P < 0.001$) rats (data not shown).⁶³

UPLC–MS analysis reproducibly detected a total of 2008 metabolite features. A cross-validated PLS-DA model was built using 2 latent factors. The resulting scores plot (Figure 2) demonstrated clear differentiation between the RUPP and normal pregnancy profiles with an $R^2 = 0.69$ and $Q^2 = 0.63$. Permutation testing showed that the probability of a model of this quality randomly occurring was less than 0.01 (Supplementary Figure S2, Supporting Information).

Univariate hypothesis testing was performed across the 2008 detected metabolite features. With a critical p -value of 0.05, 602 metabolite features were found to have significant difference between RUPP vs normal pregnant/Sham (FDR of 9%), of which, 45 were putatively identified as “unique” endogenous metabolites.

Comparison of Venous Cord Plasma Biomarkers with RUPP Biomarkers

895 metabolite features were consistently detected in both the venous cord plasma and RUPP experiments. Figure 3 compares the significance values for these common metabolites between the cord plasma study (SGA vs Control) and RUPP plasma study (normal pregnant vs RUPP). Each point in the biplot represents one of the observed common metabolites. Each point's coordinate location (x, y), is defined by the significance of the difference in mean metabolite concentration for the given case/control hypothesis test ($x = \text{venous cord plasma}$; $y = \text{RUPP}$) combined with the mean direction of the difference in metabolite concentration (+ve = case > control; –ve = case < control). One-hundred ninety-three metabolite features were significantly different in both studies (22% of the total detected). Ninety-six percent of these metabolite features showed an increase in metabolite level for the cases, with respect to control, in the RUPP model and a decrease for the cases, with respect to control,

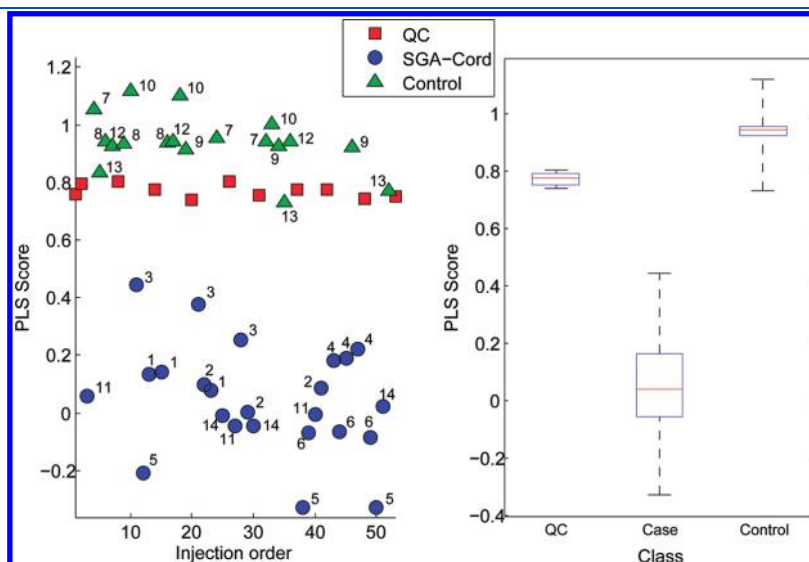


Figure 1. Cross-validated PLS-DA model of all the venous cord plasma metabolite features detected was built using two latent factors. The resulting scores plot presented as a scatter plot and box and whisker plot demonstrated clear differences between the SGA and control profiles with an $R^2 = 0.88$, $Q^2 = 0.81$, and an AUC of 1. The QC samples were not used in the model construction. These samples were simply projected through the model posthoc. The relative lack of dispersion of the projected QC samples provided robust quality assurance of the model's precision. Permutation testing showed that the probability of a model of this quality randomly occurring was less than 0.001 (Supplementary Figure S1, Supporting Information). Replicate measurements taken from the same women are numerically labeled.

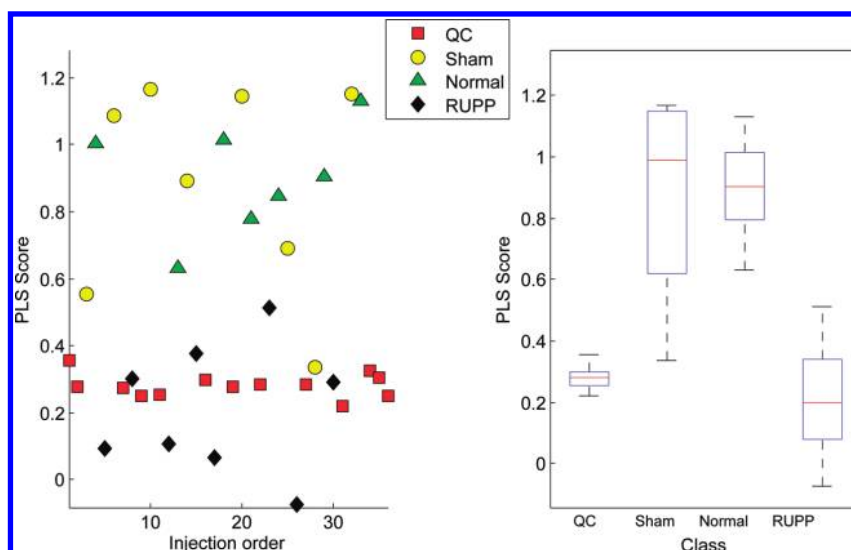


Figure 2. Cross-validated PLS-DA model of all the RUPP plasma metabolite features detected was built using 2 latent factors. The resulting scores plot presented as a scatter plot and box and whisker plot demonstrated clear differentiation between the RUPP and normal pregnancy profiles with an $R^2 = 0.69$, $Q^2 = 0.63$, and an AUC of 0.995. The QC samples were not used in the model construction. These samples were simply projected through the model posthoc. The relative lack of dispersion of the projected QC samples provided robust quality assurance of the model's precision. Permutation testing showed that the probability of a model of this quality randomly occurring was less than 0.01 (Supplementary Figure S2, Supporting Information).

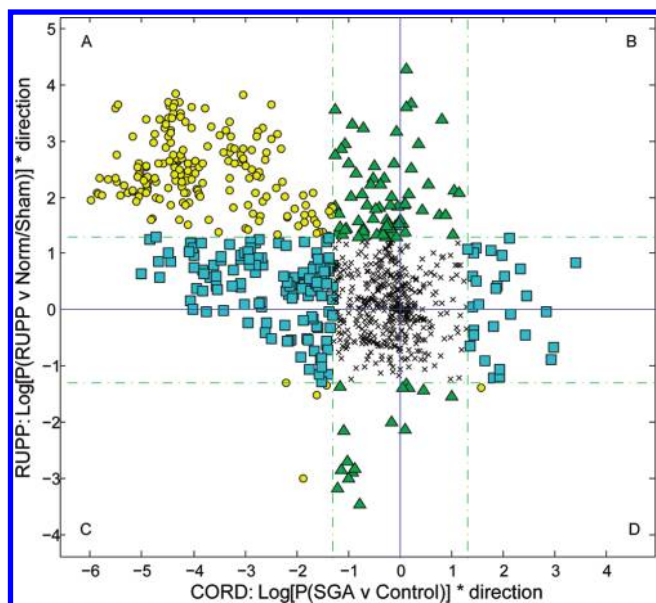


Figure 3. Eight-hundred ninety-five metabolite features were consistently detected in both the cord plasma and RUPP experiments. This biplot compares the significance values for these common metabolite features with respect to the cord plasma study (SGA vs Control) and RUPP study (Normal vs RUPP). Each point in the biplot represents one of the observed common metabolite features. A circle indicates a metabolite that significantly changes in both the venous cord plasma and RUPP significance tests. The triangles indicate metabolites that are significantly changed in RUPP but not significantly changed in venous cord plasma, and the squares indicate metabolites that are significantly changed in venous cord plasma but not significantly changed in RUPP. The crosses indicate no significant change in either the SGA or control samples. Points lying in *zone A* show a mean increase in metabolite level for RUPP samples and a mean decrease in venous cord plasma samples; *zone B* show a mean increase in metabolite level for both venous cord plasma and RUPP samples; *zone C* show a decrease in mean metabolite level for both venous cord plasma and RUPP samples; *zone D* show a decrease in mean metabolite level for RUPP samples and an increase for venous cord plasma samples.

in the cord plasma. Supplementary Table S1 (Supporting Information) lists the putatively identified metabolites that were significantly different in both studies.

Comparison of Venous Cord Plasma Biomarkers with Week-15 Peripheral Biomarkers

Maternal characteristics and pregnancy outcome of the women who subsequently delivered an SGA baby, and controls, for the week-15 peripheral plasma study are shown in Table 2. UPLC–MS analysis reproducibly detected a total of 2841 metabolite features. Seven-hundred eighty-five metabolite features were consistently detected in both the venous cord plasma and week-15 experiments. Figure 4 compares the univariate significance values for these common metabolite features with respect to the venous cord plasma study (SGA vs Control) and week-15 study (SGA vs Control).

Of the 744 metabolite features that were significant on univariate testing in the venous cord plasma experiment, 516 were also reproducibly detected in maternal peripheral plasma at 15 weeks' gestation. A cross-validated PLS-DA model (3 latent variables) constructed for the week-15 data, using only those 516 candidate SGA biomarkers, produced a $Q^2 = 0.48$, $R^2 = 0.43$, AUC of 0.94 and an optimal discriminatory odds ratio of 49 (95% CI 13–184) (Supplementary Figure S3a, Supporting Information). Permutation testing showed that the probability of a model of this quality randomly occurring was less than 0.02 (Supplementary Figure S3b, Supporting Information).

Twenty-nine metabolite features were significantly different in both studies ($p < 0.05$), of which 6 were putatively identified as “unique” endogenous metabolites (after removing the multiple matches for chemical adducts and isotope peaks). These are listed in Table 3.

Week-15 Peripheral Biomarker Signature

To find a simple, yet robust, predictive algorithm for SGA diagnosis, the data from both the venous cord plasma and week-15 studies were mined using a Genetic Algorithm-based search

Table 2. Characteristics and Pregnancy Outcome of Women Who Later Developed SGA and Controls in the Week-15 Study^a

	SGA <i>n</i> = 40	controls <i>n</i> = 40	<i>p</i> -value
Maternal Characteristics			
Age (years)	23.4 (5.4)	24.2 (5.2)	0.49
Ethnicity			
- Caucasian	39 (97.5)	39 (97.5)	1.0
- Other	1 (2.5)	1 (2.5)	
At 15 weeks gestation			
Body mass index (kg/m ²)	25.0 (4.5)	23.8 (3.8)	0.21
Systolic blood pressure (mmHg)	109 (9)	107 (10)	0.49
Diastolic blood pressure (mmHg)	64 (8)	62 (7)	0.26
Current smoker	15 (37.5%)	6 (15%)	0.02
Gestation at blood sampling (wks)	14.9 (0.7)	15.0 (0.7)	0.87
Pregnancy Outcome			
Systolic blood pressure (mmHg)	129 (15)	121 (8)	0.006
Diastolic blood pressure (mmHg)	76 (9)	74 (6)	0.23
Gestational hypertension	8 (13%)		
Gestation at delivery (wks)	39.6 (1.6)	40.2 (1.0)	0.05
Preterm Delivery (<37 wks)	3 (7.5%)		0.24
Birthweight (g)	2608 (309)	3624 (359)	<0.0001
Customized birthweight centile	4 (2, 6)	62 (44, 76)	<0.0001

^a Values are mean (SD), median (interquartile range) or number (%).

algorithm to find the subset of named metabolites that produced the most robust predictive general model. The Genetic Algorithm chose 19 metabolites (Table 4). Figure 5(a and b) shows the PLS-DA model predictions using these metabolites for both the week-15 study and the venous cord plasma study. For the week-15 data, the 19 metabolite model had an $R^2 = 0.61$, $Q^2 = 0.56$, an AUC of 0.90 and an optimal odds ratio of 44 (95% CI 9 – 214). For the venous cord plasma data the 19 metabolite model had an $R^2 = 0.83$, $Q^2 = 0.81$, and an AUC of 1. Permutation testing showed that the probability of either of these models randomly occurring was less than 0.001 (Supplementary Figure S4, Supporting Information). Of the 19 signature metabolites, 11 were also detected in the RUPP model study. The PLS-DA RUPP model built using only these metabolites gave an $R^2 = 0.66$, $Q^2 = 0.65$, and an AUC of 0.98 (Figure 5c). Again, permutation testing showed that the probability of models of this quality randomly occurring is less than 0.001 (Supplementary Figure S4, Supporting Information).

DISCUSSION

Accumulating evidence suggests that small for gestational age is a complex syndrome with multiple biological pathways contributing to the etiology. We have, therefore, taken a holistic and data-driven, systems biology approach⁸⁸ to identify a metabolic signature in plasma that is predictive of SGA. We hypothesized that widespread alterations of peripheral plasma precede the clinical onset of SGA, and that these alterations would be reflected by correlated changes in metabolite levels in cord venous plasma from affected cases. The overall study comprised of three consecutive independent studies: (a) time-of-disease biomarker discovery in cord blood plasma originating from the placenta,

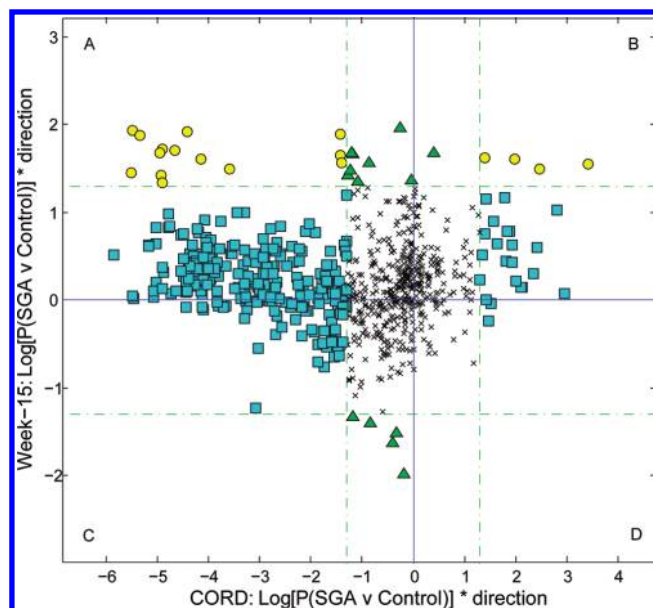


Figure 4. Seven-hundred eighty-five metabolite features were consistently detected in both the venous cord plasma and week-15 experiments. The biplot compares the univariate significance values for these common metabolite features. Each point in the biplot represents one of the observed common metabolite features with respect to the venous cord plasma study (SGA vs Control) and week-15 study (SGA vs Control). A circle indicates a metabolite that significantly changes in both the venous cord plasma and week-15 significance tests. The triangles indicate metabolites that are significantly changed in week-15 but not significantly changed in venous cord plasma, and the squares indicate metabolites that are significantly changed in venous cord plasma but not significantly changed in week-15. The crosses indicate no significant change in either the venous cord plasma or week-15 samples. Points lying in *zone A* show a mean increase in metabolite level for week-15 samples and a mean decrease in venous cord plasma samples; *zone B* show a mean increase in metabolite level for both venous cord plasma and week-15 samples; *zone C* show a decrease in mean metabolite level for both venous cord plasma and week-15 samples; *zone D* show a decrease in mean metabolite level for week-15 samples and an increase for venous cord plasma samples.

(b) biomarker validation in an animal model (c) validation of biomarkers in a presymptomatic clinical setting.

Using robust data mining and modeling techniques in these three independent studies, we have shown that a combination of 19 metabolites representing the latent systems-wide interaction in the metabolome is sufficient to produce a robust predictive model of presymptomatic SGA with an AUC of 0.9 (Figure 5). The efficacy of these 19 metabolites is also seen in the venous cord plasma and, for those detected (11 of the 19) in the RUPP model. For all of the studies, any given individual metabolite from this panel is not highly significant; however, when these metabolites are combined into a single multifactorial model, the power of such data-driven technology proves its worth. The need for such a multifactorial approach reflects the high probability that complex diseases such as SGA have more than one cause.

(a). Time-of-Disease Biomarker Discovery

Metabolic profiling of venous umbilical cord plasma revealed comprehensive disruption of plasma metabolism when comparing SGA babies with normal weight controls. Multivariate

Table 3. Putatively Identified Metabolites That Were Significant ($p < 0.05$) in Venous Cord Plasma and the Week-15 Plasma Studies^a

putative metabolite identity based on exact mass	venous cord plasma		week-15 plasma	
	<i>p</i> -value	direction	<i>p</i> -value	direction
Pregnanediol-3-glucuronide OR 3 α ,20 α -dihydroxy-5 β -pregnane 3-glucuronide	0.008	DOWN	0.003	UP
LysoPC(16:1) OR Cervonyl carnitine	1.10×10^{-5}	DOWN	0.021	UP
6-hydroxy sphingosine OR (4OH,8Z,t18:1) OR 3 β -Allotetrahydrocortisol OR 15-methyl-15-PGD2 OR 15R-PGE2 methyl ester	0.001	DOWN	0.026	UP
Leucyl-leucyl-norleucine OR Sphingosine 1-phosphate	0.040	DOWN	0.028	UP
Cervonyl carnitine AND/OR 1 α ,25-dihydroxy-18-oxocholecalciferol	3.09×10^{-6}	DOWN	0.035	UP
17-[(Benzylamino)methyl]estra-1,3,5(10)-triene-3,17 β -diol	2.68×10^{-4}	DOWN	0.045	UP

^a PC, phosphocholine; PGD, Prostaglandin D; PGE, prostaglandin E.

Table 4. Putatively Identified Metabolites That Were Used in the Final 19 Metabolite Predictive Venous Cord Plasma and Week-15 Plasma Models. *P*-values for those metabolites detected in the RUPP model are included for comparison

putative metabolite identity based on exact mass ^a	HMDB class	venous cord plasma		week-15 plasma		RUPP plasma	
		<i>p</i> -value	direction	<i>p</i> -value	direction	<i>p</i> -value	direction
Phenylacetylglutamine OR Formyl-N-acetyl-5-methoxykynurenamine	Amino Acids OR Amino Ketones	0.15	DOWN	0.06	DOWN		
Leucyl-leucyl-norleucine OR Sphingosine 1-phosphate	Amino Acids OR Sphingolipids	0.04	DOWN	0.03	UP	0.19	UP
Cervonyl carnitine AND/OR 1 α ,25-dihydroxy-18-oxocholecalciferol	Carnitines OR Vitamin D derivatives	3.09×10^{-6}	DOWN	0.004	UP	0.04	UP
(15Z)-Tetracosenoic acid OR 10,13-Dimethyl-11-docosyne-10,13-diol OR trans-selacholeic acid	Fatty Acids	0.006	DOWN	0.28	UP	0.02	UP
Hexacosanedioic acid	Fatty Acids	0.02	DOWN	0.19	UP		
Pentacosenoic acid OR Teasterone OR Typhasterol	Fatty Acids	0.02	DOWN	0.21	UP		
Cycloheptanecarboxylic acid OR Cyclohexyl acetate OR Octenoic acid OR Methyl-heptenoic acid OR 4-hydroxy-2-octenal OR DL-2-Aminooctanoic acid OR 3-amino-octanoic acid	Fatty Acids OR Amino Acids	0.09	DOWN	0.07	UP		
DG(32:0)	Glycerolipids	0.01	UP	0.39	UP	0.09	UP
LysoPC(18:2)	Glycerolipids	2.27×10^{-6}	DOWN	0.37	DOWN	0.005	DOWN
Hydroxybutyrate OR Hydroxy-methylpropanoate OR Methyl methoxyacetate	Hydroxy Acids	0.08	DOWN	0.08	UP	0.23	UP
LysoPC and PC - more than 10 hits	Phosphocholine	6.57×10^{-6}	DOWN	0.25	UP	0.001	UP
PC - more than 20 hits	Phosphocholine	0.08	DOWN	0.04	DOWN		
PC OR ubiquinone-8	Phosphocholine	0.01	DOWN	0.2	DOWN	0.66	DOWN
Acetylleucyl-leucyl-norleucinal OR Oleoylglycerone phosphate OR LPA(0:0/18:2(9Z,12Z)) OR 1-16:1-lysoPE OR PC(O-11:1(10E)/2:0) OR (3s)-3,4-Di-N-Hexanoyloxybutyl-1-Phosphocholine OR N-(3-hydroxy-propyl) arachidonoyl amine OR N-(2-methoxy-ethyl) arachidonoyl amine OR N-methyl N-(2-hydroxy-ethyl) arachidonoyl amine OR SIMILAR	Phospholipids			0.08	UP		
LysoPC(16:1) OR Cervonyl carnitine	Phospholipids OR Carnitines	1.10×10^{-5}	DOWN	0.02	UP	0.005	UP
Sphinganine 1-phosphate	Sphingolipids	0.14	DOWN	0.03	UP	0.09	UP
Sphingosine 1-phosphate	Sphingolipids	0.08	DOWN	0.05	UP	0.58	UP
Pregnanediol-3-glucuronide OR 3 α ,20 α -dihydroxy-5 β -pregnane 3-glucuronide	Steroid conjugates	0.008	DOWN	0.003	DOWN		
6-hydroxy sphingosine OR (4OH,8Z,t18:1) sphingosine OR 15-methyl-15-PGD2 OR 15R-PGE2 met, hyl ester	Steroids and Steroid Derivatives	0.001	DOWN	0.02	UP		

^a DG, Diglyceride; PC, Phosphocholine; PGD, Prostaglandin D; PGE, prostaglandin E.

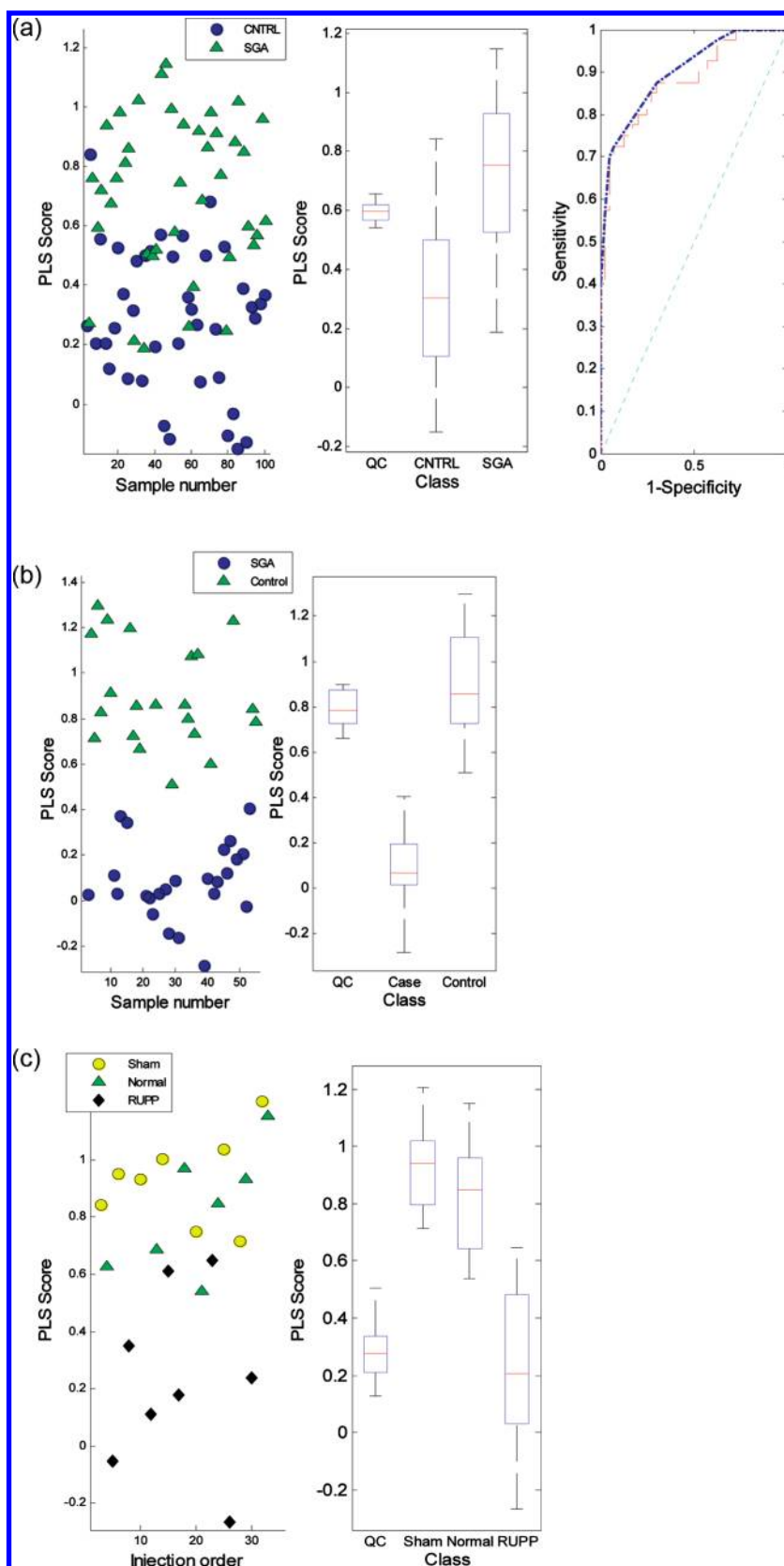


Figure 5. PLS-DA model predictions for the final 19-metabolite signature found by the Genetic Algorithm search program. (a) Model predictions for the week-15 plasma data. $R^2 = 0.61$, $Q^2 = 0.56$, an AUC of 0.90 and an optimal odds ratios of 44 (95% CI 9 – 214). (b) Model predictions for the venous cord plasma data. $R^2 = 0.83$, $Q^2 = 0.81$, and an AUC of 1. (c) Of 19 signature metabolites 11 were detected in the RUFP model analysis. The PLS-DA model built using these metabolites gave an $R^2 = 0.66$, $Q^2 = 0.65$, and an AUC of 0.98. Permutation testing showed that the probability of models of this quality randomly occurring is less than 0.001 in all cases (Supplementary Figure S4).

modeling revealed a predictive sensitivity of 1, and specificity of 1. By assessing SGA at time-of-disease and as close as possible to the hypothesized placental (dys)functional mechanism, we have uncovered evidence of a systemic change in metabolism due to this condition. It is important to note that clinical variables such as model of delivery, ethnicity, and lifestyle (see Table 1) were not controlled in this study (although matched between cases and controls). In addition no dietary constraints were imposed on the participating women. These variables have the potential of being confounding factors. However, even in a relatively small sample population, any confounding effects did not diminish the significance of the overwhelming system-wide disruption of the plasma metabolome associated with SGA at time-of-disease. Thus, we can postulate that the metabolic signature uncovered is likely to be associated with the disease state alone. This conclusion is substantiated by the correlated results found in the two subsequent studies.

(b). Biomarker Validation in an Animal Model

Comprehensive disruption of metabolism was also observed when comparing the metabolic profiles in plasma of RUPP with normal pregnant rats. When the venous cord plasma biomarker signature was compared to the RUPP biomarker signature there was significant correlation between the two experiments (Figure 3). From this figure, it is also clear that, irrespective of significance, the majority of the detected change in the respective metabolome shows a reduction in metabolite levels due to SGA in cord plasma and systemic elevation in the same metabolites due to reduced uterine perfusion pressure in rat plasma (quadrant A). This differential change may well reflect that the sampling locations were on either side of the placental barrier at time-of-disease. The “mirror image” responses may be indicative of the failure of the placenta to regulate the required nutrients and oxygen needed for successful fetal growth and development. Placental dysfunction may reduce the essential metabolites passing through the placental-barrier to the fetus, and the excess dissipated back into maternal blood; thus increasing the detected metabolite levels in maternal SGA plasma. For the metabolites that were detected in the RUPP plasma study there was no significant association with the stress of the experimental procedure (i.e., between sham and controls). This finding is also reflected in the PLS-DA model (Figure 2 and Figure 5c) where there is no significant difference between the sham and control populations with respect to the predicted PLS scores. This result is substantiated by the fact that the sham operated rats had exactly the same pup weights as the control group, suggesting that surgery per se has no lasting metabolic consequences.

A number of the putatively identified metabolites in both cord and RUPP plasma demonstrated disruption in carnitine metabolism (Supplementary Table 1, Supporting Information). These were all decreased in cord and increased in RUPP plasma. Carnitine is an essential factor in fatty acid metabolism in mammals. Its most important known metabolic function is to transport fatty acids into the mitochondria of cells for oxidation.⁸⁹ The placenta has a high activity of fatty acid oxidation enzymes⁹⁰ and where defects in long-chain fatty acid oxidation are noted, there is a higher frequency of SGA.⁹¹ Previous studies have also found reduced levels of carnitine and acylcarnitines in cord blood of SGA infants.^{92,93} Other rat studies of placental insufficiency have reported down-regulated insulin receptor and reduced expression of enzymes involved in fatty acid formation and oxidation as well as altered skeletal muscle mitochondrial lipid metabolism in

the growth-restricted pups.^{94,95} These metabolic changes may also play a role in the long term effects associated with SGA.

(c). Biomarker Validation in a Presymptomatic Clinical Setting

When the biomarker signature of SGA in cord plasma was investigated in peripheral blood collected at 15 ± 1 weeks' gestation, the disruption of metabolism was consistent with the previous two studies; however, the change in metabolism was less severe. Only 29 metabolite features were significant after univariate testing in both the cord plasma and week-15 studies (6 identified – Table 3); however, irrespective of significance, Figure 4 shows that there is a clear trend for metabolites to have reduced levels in the cord plasma and elevated levels in the peripheral maternal plasma. These findings were consistent with the comparison of cord plasma with RUPP plasma (Figure 3). This would again suggest that the source of this disruption is at the placental level.

(d). Nineteen Metabolite Signature of SGA Across All Three Studies

Finally, a 19 named metabolomic signature of presymptomatic SGA was uncovered using a Genetic-Algorithm search program, utilizing both the venous cord plasma and week-15 data. The final panel of metabolites proved effective at discriminating SGA plasma from controls in both the presymptomatic week-15 (AUC = 0.9) and the venous cord plasma data. This suggests that the phenotype of SGA is not only multifactorial, (especially so, early in pregnancy), but that ultimately, metabolomic analysis may provide a predictive early screening test for SGA.

A number of sphingolipids were among this panel of metabolites. Sphingolipids are ubiquitous in mammals, playing important roles in signal transmission and cell recognition and are commonly believed to protect the cell surface against harmful environmental factors by forming a mechanically stable and chemically resistant outer leaflet of the plasma membrane lipid bilayer. In particular, sphingosine 1-phosphate (S1P) has been shown to be an important mediator in the signaling cascades involved in apoptosis, proliferation and stress responses.^{96,97} It is also known that growth restriction is associated with increased apoptosis and reduced cytotrophoblast proliferation.^{30,31}

Phospholipids also showed significant disruption. Phospholipids are the major lipid constituents of cell membranes. Changes in normal oxygen tensions, which are associated with the pathophysiology of SGA, can cause changes to glycerophosphatidylipids resulting in many different products which have many different proposed biological properties.⁹⁸ The phospholipid changes observed in this study are most likely a result of cell membrane damage leading to the subsequent release of phospholipids. However, there is recent evidence of antiphospholipid antibodies (and complement activation) co-operating in triggering a local inflammatory process, eventually leading to placental thrombosis, hypoxia, and neutrophil infiltration.⁹⁹

SGA and Fetal Growth Restriction. The metabolites from the 19-metabolite SGA panel that were detected in the RUPP study (11 of the 19 metabolites) were tested for their multifactorial discriminatory power in the RUPP plasma samples. With a PLS-DA AUC of 0.98, it is probable that there is some causal connection between the SGA metabolite signature and the rat model of severe growth restriction. This is reinforced by the high number of overlapping significant metabolites in the comparison of RUPP to venous cord plasma (Figure 3; Supplementary Table 1, Supporting Information).

Fetal growth restriction (FGR) is defined as failure of a fetus to achieve its genetically determined potential size. Currently, classifying babies as growth restricted with a high degree of specificity and sensitivity is a complex process, and is difficult to measure in a general clinical setting. It is common practice for SGA to be used as the surrogate end point for FGR.^{9,100} However, not all fetuses that are SGA are pathologically growth restricted and, in fact, as many as 30% may be constitutionally small.¹¹ Therefore, we recognize that there are limitations in the use of the birth weight percentile as a surrogate marker of FGR.

It is possible, given the evidence presented here, that we have in fact found a metabolic signature for FGR rather than the more general disease classification SGA. This hypothesis is reinforced by examining the prediction scores of the 19-metabolite PLS-DA model for the week-15 plasma (Figure 5a). Although, as a general measure of quality an AUC = 0.9 is excellent, it can readily be seen from the predictive scatter plot that several SGA samples are misclassified. Of note, the “misclassification rate” of 30% is close to the estimated misclassification rate using SGA as the end point for FGR discussed above.

One potential limitation of this study is the number of smokers (SGA = 15; Controls = 6) and the number of SGA women with Gestational Hypertension ($n = 8$) in the week-15 Adelaide study. Population matching was performed as rigorously as possible; however, our nested case-control study was limited by the size of the overall SCOPE prospective cohort, and excluding these participants would have significantly reduced the power of the study. Moreover, one of the main objectives of our work is to develop a screening test that performs robustly in all populations. The predictive ability of the final model (combined with agreement with the venous cord blood and RUPP studies) clearly outweighs any possible confounding influence of the above factors.

CONCLUSIONS

This combined study clearly illustrates the utility of integrating metabolomic analysis of different sample types when investigating diseases/syndromes which are believed to have complex multifactorial etiologies. The unambiguous identification of potential biomarkers at time-of-disease, and thus as close to the clinical end point as possible, followed by validation using an animal model with known causality, provided the reasoning for their further investigation in maternal blood at an early, and hence clinically useful, time point. The dramatic metabolic differences of sampling at opposite sides of the placenta are also demonstrated giving support to the evidence that the disruption is at the placental level.

This is the first time any clear biomarkers for SGA have been discovered using any technology. Ongoing metabolomics work with a larger prospective cohort of healthy nulliparous women will further validate the predictive model. A presymptomatic predictive test in early pregnancy will have a significant impact on clinical care, streamlining surveillance to those deemed to be at higher risk. Such a test and greater understanding of the pathophysiology will provide the basis for developing therapeutic interventions that could minimize the likelihood of serious complications later in pregnancy and throughout life.

ASSOCIATED CONTENT

Supporting Information

Supplementary detailed methodological procedures. Table S1. The putatively identified metabolites that were significantly

different between the cord plasma study (SGA vs Control) and RUPP plasma study (Normal vs RUPP). Figure S1. Permutation test comparing the PLS-DA model of all the venous cord plasma metabolite features detected and the permuted H_0 distribution. Figure S2. Permutation test comparing the PLS-DA model of all the RUPP plasma metabolite features detected and the permuted H_0 distribution. Figure S3. PLS-DA model constructed using the week-15 data, using only those metabolites that previously showed significant difference in the VCP study and were reproducibly detected in the week-15 study. Permutation test comparing this model and the permuted H_0 distribution. Figure S4. Permutation test comparing the PLS-DA model predictions for the 19-metabolite signature and the permuted H_0 distribution for (a) the week-15 plasma, (b) the venous cord plasma and (c) the RUPP plasma. This material is available free of charge via the Internet at <http://pubs.acs.org>.

AUTHOR INFORMATION

Corresponding Author

*Prof. Louise C. Kenny, E-mail l.kenny@ucc.ie, Tel +353 (0)21 420 5023, Fax +353 (0)21 420 5025.

ACKNOWLEDGMENT

We thank the SCOPE Consortium for the use of the early pregnancy plasma samples and the midwives on Central Delivery Unit, St Mary's Hospital, Manchester for their assistance in acquiring cord blood samples and the patients for consenting for same. R.P.H. is funded by the Health Research Board and Health Service Executive of Ireland (CRT/2007/5). S.K.W. was supported by Science Foundation Ireland grant (SFI 07/RFP/BIMF796). L.C.K. is a Health Research Board Clinician Scientist (CSA/2007/2) and a Science Foundation Ireland Principal Investigator (08/IN.1/B2083). The funding bodies did not have any involvement in the preparation of this article. W.D. thanks BBSRC and EPSRC for financial support of The Manchester Centre for Integrative Systems Biology and the NIHR for financial support of The Manchester Biomedical Research Centre.

REFERENCES

- (1) Morrison, I.; Olsen, J. Weight-Specific Stillbirths and Associated Causes of Death - an Analysis of 765 Stillbirths. *Am. J. Obstet. Gynecol.* **1985**, *152* (8), 975–980.
- (2) Gardosi, J.; Kady, S. M.; McGeown, P.; Francis, A.; Tonks, A. Classification of stillbirth by relevant condition at death (ReCoDe): population based cohort study. *Br. Med. J.* **2005**, *331* (7525), 1113–1117.
- (3) Low, J. A.; Handleyderry, M. H.; Burke, S. O.; Peters, R. D.; Pater, E. A.; Killen, H. L.; Derrick, E. J. Association of Intrauterine Fetal Growth-Retardation and Learning-Deficits at Age 9 to 11 Years. *Am. J. Obstet. Gynecol.* **1992**, *167* (6), 1499–1505.
- (4) Kok, J. H.; den Ouden, A. L.; Verloove-Vanhorick, S. P.; Brand, R. Outcome of very preterm small for gestational age infants: the first nine years of life. *Br. J. Obstet. Gynaecol.* **1998**, *105* (2), 162–168.
- (5) Barker, D. J. P.; Gluckman, P. D.; Godfrey, K. M.; Harding, J. E.; Owens, J. A.; Robinson, J. S. Fetal Nutrition and Cardiovascular-Disease in Adult Life. *Lancet* **1993**, *341* (8850), 938–941.
- (6) Saenger, P.; Czernichow, P.; Hughes, I.; Reiter, E. O. Small for gestational age: short stature and beyond. *Endocr. Rev.* **2007**, *28* (2), 219–251.
- (7) Gluckman, P. D.; Hanson, M. A.; Cooper, C.; Thornburg, K. L. Effect of in utero and early-life conditions on adult health and disease. *N. Engl. J. Med.* **2008**, *359* (1), 61–73.

- (8) Barker, D. J. P.; Eriksson, J. G.; Forsen, T.; Osmond, C. Fetal origins of adult disease: strength of effects and biological basis. *Int. J. Epidemiol.* **2002**, *31* (6), 1235–1239.
- (9) RCOG. *The investigation and management of the small-for-gestational-age fetus*. Evidence-based Clinical Guideline No. 31; RCOG Press: London, 2002; pp 1–16.
- (10) Gardosi, J.; Chang, A.; Kalyan, B.; Sahota, D.; Symonds, E. M. Customized Antenatal Growth Charts. *Lancet* **1992**, *339* (8788), 283–287.
- (11) McCowan, L. M.; Harding, J. E.; Stewart, A. W. Customized birthweight centiles predict SGA pregnancies with perinatal morbidity. *Br. J. Obstet. Gynaecol.* **2005**, *112* (8), 1026–1033.
- (12) Chang, T. C.; Robson, S. C.; Boys, R. J.; Spencer, J. A. D. Prediction of the Small-for-Gestational-Age Infant - Which Ultrasonic Measurement Is Best. *Obstet. Gynecol.* **1992**, *80* (6), 1030–1038.
- (13) Hall, M. H.; Chng, P. K.; MacGillivray, I. Is routine antenatal care worth while? *Lancet* **1980**, *2* (8185), 78–80.
- (14) Gardosi, J.; Francis, A. Controlled trial of fundal height measurement plotted on customised antenatal growth charts. *Br. J. Obstet. Gynaecol.* **1999**, *106* (4), 309–317.
- (15) Bhatia, S.; Faessen, G. H.; Carland, G.; Balise, R. L.; Gargosky, S. E.; Druzin, M.; El-Sayed, Y.; Wilson, D. M.; Giudice, L. C. A longitudinal analysis of maternal serum insulin-like growth factor I (IGF-I) and total and nonphosphorylated IGF-binding protein-1 in human pregnancies complicated by intrauterine growth restriction. *J. Clin. Endocrinol. Metab.* **2002**, *87* (4), 1864–1870.
- (16) Tjoa, M. L.; Mulders, M. A.; van Vugt, J. M.; Blankenstein, M. A.; Oudejans, C. B.; van Wijk, I. J. Plasma hepatocyte growth factor as a marker for small-for-gestational age fetuses. *Eur. J. Obstet. Gynecol. Reprod. Biol.* **2003**, *110* (1), 20–25.
- (17) Dugoff, L.; Hobbins, J. C.; Malone, F. D.; Porter, T. F.; Luthy, D.; Comstock, C. H.; Hankins, G.; Berkowitz, R. L.; Merkatz, I.; Craigo, S. D.; Timor-Tritsch, I. E.; Carr, S. R.; Wolfe, H. M.; Vidaver, J.; D'Alton, M. E. First-trimester maternal serum PAPP-A and free-beta subunit human chorionic gonadotropin concentrations and nuchal translucency are associated with obstetric complications: a population-based screening study (the FASTER Trial). *Am. J. Obstet. Gynecol.* **2004**, *191* (4), 1446–1451.
- (18) Dugoff, L.; Hobbins, J. C.; Malone, F. D.; Vidaver, J.; Sullivan, L.; Canick, J. A.; Lambert-Messerlian, G. M.; Porter, T. F.; Luthy, D. A.; Comstock, C. H.; Saade, G.; Eddleman, K.; Merkatz, I. R.; Craigo, S. D.; Timor-Tritsch, I. E.; Carr, S. R.; Wolfe, H. M.; D'Alton, M. E. Quad screen as a predictor of adverse pregnancy outcome. *Obstet. Gynecol.* **2005**, *106* (2), 260–267.
- (19) Morris, R. K.; Nossen, J. S.; Langejans, M.; Robson, S. C.; Kleijnen, J.; Ter Riet, G.; Mol, B. W.; van der Post, J. A.; Khan, K. S. Serum screening with Down's syndrome markers to predict pre-eclampsia and small for gestational age: systematic review and meta-analysis. *BMC Pregnancy Childbirth* **2008**, *8*, 33.
- (20) Bersinger, N. A.; Odegard, R. A. Second- and third-trimester serum levels of placental proteins in preeclampsia and small-for-gestational age pregnancies. *Acta Obstet. Gynecol. Scand.* **2004**, *83* (1), 37–45.
- (21) Bersinger, N. A.; Odegard, R. A. Serum levels of macrophage colony stimulating, vascular endothelial, and placenta growth factor in relation to later clinical onset of pre-eclampsia and a small-for-gestational age birth. *Am. J. Reprod. Immunol.* **2005**, *54* (2), 77–83.
- (22) Taylor, R. N.; Grimwood, J.; Taylor, R. S.; McMaster, M. T.; Fisher, S. J.; North, R. A. Longitudinal serum concentrations of placental growth factor: Evidence for abnormal placental angiogenesis in pathologic pregnancies. *Am. J. Obstet. Gynecol.* **2003**, *188* (1), 177–182.
- (23) Bamberg, C.; Kalache, K. D. Prenatal diagnosis of fetal growth restriction. *Semin. Fetal Neonatal Med.* **2004**, *9* (5), 387–394.
- (24) McCowan, L.; Horgan, R. P. Risk factors for small for gestational age infants. *Best Pract. Res. Clin. Obstet. Gynaecol.* **2009**, *23* (6), 779–793.
- (25) Kingdom, J.; Huppertz, B.; Seaward, G.; Kaufmann, P. Development of the placental villous tree and its consequences for fetal growth. *Eur. J. Obstet. Gynecol. Reprod. Biol.* **2000**, *92* (1), 35–43.
- (26) Gagnon, R. Placental insufficiency and its consequences. *Eur. J. Obstet. Gynecol. Reprod. Biol.* **2003**, *110*, S99–S107.
- (27) Trudinger, B. J.; Giles, W. B. Elaboration of stem villous vessels in growth restricted pregnancies with abnormal umbilical artery Doppler waveforms. *Br. J. Obstet. Gynaecol.* **1996**, *103* (5), 487–488.
- (28) Jackson, M. R.; Walsh, A. J.; Morrow, R. J.; Mullen, J. B. M.; Lye, S. J.; Ritchie, J. W. Reduced placental villous tree elaboration in small-for-gestational-age pregnancies - relationship with umbilical artery Doppler wave-forms. *Am. J. Obstet. Gynecol.* **1995**, *172* (2), 518–525.
- (29) Scifres, C. M.; Nelson, D. M. Intrauterine growth restriction, human placental development and trophoblast cell death. *J. Physiol.* **2009**, *587* (Pt 14), 3453–3458.
- (30) Smith, S. C.; Baker, P. N.; Symonds, E. M. Increased placental apoptosis in intrauterine growth restriction. *Am. J. Obstet. Gynecol.* **1997**, *177* (6), 1395–1401.
- (31) Chen, C. P.; Bajoria, R.; Aplin, J. D. Decreased vascularization and cell proliferation in placentas of intrauterine growth-restricted fetuses with abnormal umbilical artery flow velocity waveforms. *Am. J. Obstet. Gynecol.* **2002**, *187* (3), 764–769.
- (32) Harrigan, G. G.; Goodacre, R. *Metabolic profiling: its role in biomarker discovery and gene function analysis*; Kluwer Academic Publishers: Boston, 2003.
- (33) Allen, J.; Davey, H. M.; Broadhurst, D.; Heald, J. K.; Rowland, J. J.; Oliver, S. G.; Kell, D. B. High-throughput classification of yeast mutants for functional genomics using metabolic footprinting. *Nat. Biotechnol.* **2003**, *21* (6), 692–696.
- (34) Dunn, W. B.; Broadhurst, D. I.; Atherton, H. J.; Goodacre, R.; Griffin, J. L. Systems level studies of mammalian metabolomes: the roles of mass spectrometry and nuclear magnetic resonance spectroscopy. *Chem. Soc. Rev.* **2011**, *40* (1), 387–426.
- (35) Fiehn, O. Extending the breadth of metabolite profiling by gas chromatography coupled to mass spectrometry. *Trends Anal. Chem.* **2008**, *27* (3), 261–269.
- (36) Denkert, C.; Budczies, J.; Kind, T.; Weichert, W.; Tablack, P.; Sehouli, J.; Niesporek, S.; Kongsen, D.; Dietel, M.; Fiehn, O. Mass spectrometry-based metabolic profiling reveals different metabolite patterns in invasive ovarian carcinomas and ovarian borderline tumors. *Cancer Res.* **2006**, *66* (22), 10795–10804.
- (37) Wilson, I. D.; Plumb, R.; Granger, J.; Major, H.; Williams, R.; Lenz, E. M. HPLC-MS-based methods for the study of metabolomics. *J. Chromatogr. B: Anal. Technol. Biomed. Life Sci.* **2005**, *817* (1), 67–76.
- (38) Monton, M. R.; Soga, T. Metabolome analysis by capillary electrophoresis-mass spectrometry. *J. Chromatogr. A* **2007**, *1168* (1–2), 237–246; discussion 236.
- (39) Barton, R. H.; Nicholson, J. K.; Elliott, P.; Holmes, E. High-throughput 1H NMR-based metabolic analysis of human serum and urine for large-scale epidemiological studies: validation study. *Int. J. Epidemiol.* **2008**, *37* (Suppl 1), i31–40.
- (40) Gieger, C.; Geistlinger, L.; Altmaier, E.; Hrabce de Angelis, M.; Kronenberg, F.; Meitinger, T.; Mewes, H. W.; Wichmann, H. E.; Weinberger, K. M.; Adamski, J.; Illig, T.; Suhre, K. Genetics meets metabolomics: a genome-wide association study of metabolite profiles in human serum. *PLoS Genet.* **2008**, *4* (11), e1000282.
- (41) Want, E. J.; Wilson, I. D.; Gika, H.; Theodoridis, G.; Plumb, R. S.; Shockcor, J.; Holmes, E.; Nicholson, J. K. Global metabolic profiling procedures for urine using UPLC-MS. *Nat. Protoc.* **2010**, *5* (6), 1005–1018.
- (42) Kell, D. B.; Oliver, S. G. Here is the evidence, now what is the hypothesis? The complementary roles of inductive and hypothesis-driven science in the post-genomic era. *Bioessays* **2004**, *26* (1), 99–105.
- (43) Dunn, W. B. Current trends and future requirements for the mass spectrometric investigation of microbial, mammalian and plant metabolomes. *Phys. Biol.* **2008**, *5* (1), 11001.
- (44) MacKenzie, D. A.; Defernez, M.; Dunn, W. B.; Brown, M.; Fuller, L. J.; de Herrera, S. R. M. S.; Guenther, A.; James, S. A.; Eagles, J.; Philo, M.; Goodacre, R.; Roberts, I. N. Relatedness of medically important strains of *Saccharomyces cerevisiae* as revealed by phylogenetics and metabolomics. *Yeast* **2008**, *25* (7), 501–512.

- (45) Fiehn, O.; Kopka, J.; Dormann, P.; Altmann, T.; Trethewey, R. N.; Willmitzer, L. Metabolite profiling for plant functional genomics. *Nat. Biotechnol.* **2000**, *18* (11), 1157–1161.
- (46) Holmes, E.; Loo, R. L.; Stamler, J.; Bictash, M.; Yap, I. K.; Chan, Q.; Ebbels, T.; De Iorio, M.; Brown, I. J.; Veselkov, K. A.; Daviglus, M. L.; Kesteloot, H.; Ueshima, H.; Zhao, L.; Nicholson, J. K.; Elliott, P. Human metabolic phenotype diversity and its association with diet and blood pressure. *Nature* **2008**, *453* (7193), 396–400.
- (47) Walsh, M. C.; Brennan, L.; Roche, H.; Gibney, M. J. Metabolomics as a Tool in Nutrition Intervention Studies. *Ann. Nutr. Metab.* **2009**, *55*, 445–445.
- (48) Bundy, J. G.; Davey, M. P.; Viant, M. R. Environmental metabolomics: a critical review and future perspectives. *Metabolomics* **2009**, *5* (1), 3–21.
- (49) Kenny, L. C.; Broadhurst, D. I.; Dunn, W. B.; Brown, M.; North, R. A.; McCowan, L.; Roberts, C.; Cooper, G. J. S.; Kell, D. B.; Baker, P. N. Robust early pregnancy prediction of later preeclampsia using metabolomic biomarkers. *Hypertension* **2010**, *56* (4), 741–749.
- (50) Holmes, E.; Tsang, T. M.; Huang, J. T.; Leweke, F. M.; Koethe, D.; Gerth, C. W.; Nolden, B. M.; Gross, S.; Schreiber, D.; Nicholson, J. K.; Bahn, S. Metabolic profiling of CSF: evidence that early intervention may impact on disease progression and outcome in schizophrenia. *PLoS Med.* **2006**, *3* (8), e327.
- (51) Ong, K. R.; Sims, A. H.; Harvie, M.; Chapman, M.; Dunn, W. B.; Broadhurst, D.; Goodacre, R.; Wilson, M.; Thomas, N.; Clarke, R. B.; Howell, A. Biomarkers of Dietary Energy Restriction in Women at Increased Risk of Breast Cancer. *Cancer Prev. Res.* **2009**, *2* (8), 720–731.
- (52) Sabatine, M. S.; Liu, E.; Morrow, D. A.; Heller, E.; McCarroll, R.; Wiegand, R.; Berriz, G. F.; Roth, F. P.; Gerszten, R. E. Metabolomic identification of novel biomarkers of myocardial ischemia. *Circulation* **2005**, *112* (25), 3868–3875.
- (53) Dunn, W. B.; Broadhurst, D. I.; Deepak, S. M.; Buch, M. H.; McDowell, G.; Spasic, I.; Ellis, D. I.; Brooks, N.; Kell, D. B.; Neyses, L. Serum metabolomics reveals many novel metabolic markers of heart failure, including pseudouridine and 2-oxoglutarate. *Metabolomics* **2007**, *3*, 413–426.
- (54) Sreekumar, A.; Poisson, L. M.; Rajendiran, T. M.; Khan, A. P.; Cao, Q.; Yu, J.; Laxman, B.; Mehra, R.; Lonigro, R. J.; Li, Y.; Nyati, M. K.; Ahsan, A.; Kalyana-Sundaram, S.; Han, B.; Cao, X.; Byun, J.; Omenn, G. S.; Ghosh, D.; Pennathur, S.; Alexander, D. C.; Berger, A.; Shuster, J. R.; Wei, J. T.; Varambally, S.; Beecher, C.; Chinnaiyan, A. M. Metabolomic profiles delineate potential role for sarcosine in prostate cancer progression. *Nature* **2009**, *457* (7231), 910–914.
- (55) Kell, D. B. The virtual human: Towards a global systems biology of multiscale, distributed biochemical network models. *IUBMB Life* **2007**, *59*, 689–695.
- (56) Westerhoff, H. V.; Palsson, B. O. The evolution of molecular biology into systems biology. *Nat. Biotechnol.* **2004**, *22* (10), 1249–1252.
- (57) Psychogios, N.; Hau, D. D.; Peng, J.; Guo, A. C.; Mandal, R.; Bouatra, S.; Sinelnikov, I.; Krishnamurthy, R.; Eisner, R.; Gautam, B.; Young, N.; Xia, J.; Knox, C.; Dong, E.; Huang, P.; Hollander, Z.; Pedersen, T. L.; Smith, S. R.; Bamforth, F.; Greiner, R.; McManus, B.; Newman, J. W.; Goodfriend, T.; Wishart, D. S. The human serum metabolome. *PLoS One* **2011**, *6* (2), e16957.
- (58) Dunn, W. B.; Broadhurst, D.; Ellis, D. I.; Brown, M.; Halsall, A.; O'Hagan, S.; Spasic, I.; Tseng, A.; Kell, D. B. A GC-TOF-MS study of the stability of serum and urine metabolomes during the UK Biobank sample collection and preparation protocols. *Int. J. Epidemiol.* **2008**, *37* (Suppl 1), i23–30.
- (59) Zelena, E.; Dunn, W. B.; Broadhurst, D.; Francis-McIntyre, S.; Carroll, K. M.; Begley, P.; O'Hagan, S.; Knowles, J. D.; Halsall, A.; Wilson, I. D.; Kell, D. B. Development of a robust and repeatable UPLC-MS method for the long-term metabolomic study of human serum. *Anal. Chem.* **2009**, *81* (4), 1357–1364.
- (60) Kenny, L. C.; Dunn, W. B.; Ellis, D. I.; Myers, J.; Baker, P. N.; Kell, D. B. Consortium, G., Novel biomarkers for pre-eclampsia detected using metabolomics and machine learning. *Metabolomics* **2005**, *1* (3), 227–234.
- (61) Kenny, L. C.; Broadhurst, D.; Brown, M.; Dunn, W. B.; Redman, C. W. G.; Kill, D. B.; Baker, P. N. Detection and identification of novel metabolomic biomarkers in preeclampsia. *Reprod. Sci.* **2008**, *15* (6), 591–597.
- (62) Turner, E.; Brewster, J. A.; Simpson, N. A.; Walker, J. J.; Fisher, J. Aromatic amino acid biomarkers of preeclampsia—a nuclear magnetic resonance investigation. *Hypertens. Pregnancy* **2008**, *27* (3), 225–235.
- (63) Walsh, S. K.; English, F. A.; Johns, E. J.; Kenny, L. C. Plasma-mediated vascular dysfunction in the reduced uterine perfusion pressure model of preeclampsia: a microvascular characterization. *Hypertension* **2009**, *54* (2), 345–351.
- (64) Alexander, B. T. Placental insufficiency leads to development of hypertension in growth-restricted offspring. *Hypertension* **2003**, *41* (3), 457–462.
- (65) Anthony, R. V.; Scheaffer, A. N.; Wright, C. D.; Regnault, T. R. Ruminant models of prenatal growth restriction. *Reprod. Suppl.* **2003**, *61*, 183–194.
- (66) Ergaz, Z.; Avgil, M.; Ornoy, A. Intrauterine growth restriction—etiology and consequences: what do we know about the human situation and experimental animal models? *Reprod. Toxicol.* **2005**, *20* (3), 301–322.
- (67) Eder, D. J.; McDonald, M. T. A role for brain angiotensin-II in experimental pregnancy-induced hypertension in laboratory rats. *Clin. Exp. Hypertens. Part B: Hypertens. Pregnancy* **1988**, *6* (3), 431–451.
- (68) Nienartowicz, A.; Link, S.; Moll, W. Adaptation of the uterine arcade in rats to pregnancy. *J. Dev. Physiol.* **1989**, *12* (2), 101–108.
- (69) Broadhurst, D. I.; Kell, D. B. Statistical strategies for avoiding false discoveries in metabolomics and related experiments. *Metabolomics* **2006**, *2* (4), 171–196.
- (70) Dunn, W. B.; Broadhurst, D.; Brown, M.; Baker, P. N.; Redman, C. W. G.; Kenny, L. C.; Kell, D. B. Metabolic profiling of serum using Ultra Performance Liquid Chromatography and the LTQ-Orbitrap mass spectrometry system. *J. Chromatogr., B: Anal. Technol. Biomed. Life Sci.* **2008**, *871* (2), 288–298.
- (71) Brown, M.; Dunn, W. B.; Dobson, P.; Patel, Y.; Winder, C. L.; Francis-McIntyre, S.; Begley, P.; Carroll, K.; Broadhurst, D.; Tseng, A.; Swainston, N.; Spasic, I.; Goodacre, R.; Kell, D. B. Mass spectrometry tools and metabolite-specific databases for molecular identification in metabolomics. *Analyst* **2009**, *134* (7), 1322–1332.
- (72) Storey, J. D. A direct approach to false discovery rates. *J. R. Stat. Soc., Ser. B: Stat. Methodol.* **2002**, *64*, 479–498.
- (73) Eriksson, L.; Johansson, E.; Kettaneh-Wold, N.; Wold, S. *Multi-and megavariable data analysis: principles and applications*; Umetrics Academy: Umeå, 2001.
- (74) Wold, H. Soft Modelling by Latent Variables: The Non-Linear Iterative Partial Least Squares (NIPALS) Approach. In *Perspectives in Probability and Statistics, Papers in Honour of M. S. Bartlett*; Gani, J., Ed.; Academic Press: London, 1975; pp 117–142.
- (75) Wold, S.; Trygg, J.; Berglund, A.; Antti, H. Some recent developments in PLS modeling. *Chemom. Intell. Lab. Syst.* **2001**, *58* (2), 131–150.
- (76) Westerhuis, J. A.; Hoefsloot, H. C. J.; Smit, S.; Vis, D. J.; Smilde, A. K.; van Velzen, E. J. J.; van Duijnhoven, J. P. M.; van Dorsten, F. A. Assessment of PLS-DA cross validation. *Metabolomics* **2008**, *4* (1), 81–89.
- (77) Broadhurst, D.; Goodacre, R.; Jones, A.; Rowland, J. J.; Kell, D. B. Genetic algorithms as a method for variable selection in multiple linear regression and partial least squares regression, with applications to pyrolysis mass spectrometry. *Anal. Chim. Acta* **1997**, *348* (1–3), 71–86.
- (78) Cavill, R.; Keun, H. C.; Holmes, E.; Lindon, J. C.; Nicholson, J. K.; Ebbels, T. M. Genetic algorithms for simultaneous variable and sample selection in metabolomics. *Bioinformatics* **2009**, *25* (1), 112–118.
- (79) Jarvis, R. M.; Goodacre, R. Genetic algorithm optimization for pre-processing and variable selection of spectroscopic data. *Bioinformatics* **2005**, *21* (7), 860–868.

- (80) Kell, D. B. Metabolomics and machine learning: explanatory analysis of complex metabolome data using genetic programming to produce simple, robust rules. *Mol. Biol. Rep.* **2002**, *29* (1–2), 237–241.
- (81) Goodacre, R.; Kell, D. B. Evolutionary computation for the interpretation of metabolome data. In *Metabolic profiling: its role in biomarker discovery and gene function*; Harrigan, G. G., Goodacre, R., Eds.; Kluwer Academic Publishers: Boston, 2003; pp 239–256.
- (82) van den Berg, R. A.; Hoefsloot, H. C.; Westerhuis, J. A.; Smilde, A. K.; van der Werf, M. J. Centering, scaling, and transformations: improving the biological information content of metabolomics data. *BMC Genomics* **2006**, *7*, 142.
- (83) Speed, T. P., *Statistical analysis of gene expression microarray data*; Chapman & Hall/CRC: Boca Raton, FL, 2003; ISBN: 1584883278; pp 66–74.
- (84) Youden, W. J. Index for Rating Diagnostic Tests. *Cancer* **1950**, *3* (1), 32–35.
- (85) Perkins, N. J.; Schisterman, E. F. The inconsistency of “optimal” cutpoints obtained using two criteria based on the receiver operating characteristic curve. *Am. J. Epidemiol.* **2006**, *163* (7), 670–675.
- (86) Herrgard, M. J.; Swainston, N.; Dobson, P.; Dunn, W. B.; Arga, K. Y.; Arvas, M.; Bluthgen, N.; Borger, S.; Costenoble, R.; Heinemann, M.; Hucka, M.; Le Novere, N.; Li, P.; Liebermeister, W.; Mo, M. L.; Oliveira, A. P.; Petranovic, D.; Pettifer, S.; Simeonidis, E.; Smallbone, K.; Spasic, I.; Weichart, D.; Brent, R.; Broomhead, D. S.; Westerhoff, H. V.; Kirdar, B.; Penttila, M.; Klipp, E.; Palsson, B. O.; Sauer, U.; Oliver, S. G.; Mendes, P.; Nielsen, J.; Kell, D. B. A consensus yeast metabolic network reconstruction obtained from a community approach to systems biology. *Nat. Biotechnol.* **2008**, *26* (10), 1155–1160.
- (87) Brown, M.; Wedge, D. C.; Goodacre, R.; Kell, D. B.; Baker, P. N.; Kenny, L. C.; Mamas, M. A.; Neyses, L.; Dunn, W. B. Automated workflows for accurate mass-based putative metabolite identification in LC/MS-derived metabolomic datasets. *Bioinformatics* **2011**, *27* (8), 1108–1112.
- (88) Kell, D. B. Metabolomics and systems biology: making sense of the soup. *Curr. Opin. Microbiol.* **2004**, *7* (3), 296–307.
- (89) Borum, P. R. Carnitine in neonatal nutrition. *J. Child Neurol.* **1995**, *10* (Suppl 2), S25–31.
- (90) Oey, N. A.; den Boer, M. E.; Ruiters, J. P.; Wanders, R. J.; Duran, M.; Waterham, H. R.; Boer, K.; van der Post, J. A.; Wijburg, F. A. High activity of fatty acid oxidation enzymes in human placenta: implications for fetal-maternal disease. *J. Inherit. Metab. Dis.* **2003**, *26* (4), 385–392.
- (91) Tyni, T.; Ekholm, E.; Pihko, H. Pregnancy complications are frequent in long-chain 3-hydroxyacyl-coenzyme A dehydrogenase deficiency. *Am. J. Obstet. Gynecol.* **1998**, *178* (3), 603–608.
- (92) Meyburg, J.; Schulze, A.; Kohlmüller, D.; Linderkamp, O.; Mayatepek, E. Postnatal changes in neonatal acylcarnitine profile. *Pediatr. Res.* **2001**, *49* (1), 125–129.
- (93) Akisu, M.; Bekler, C.; Yalaz, M.; Huseyinov, A.; Kultursay, N. Free carnitine concentrations in cord blood in preterm and full-term infants with intrauterine growth retardation. *Pediatr. Int.* **2001**, *43* (1), 107–108.
- (94) Germani, D.; Puglianiello, A.; Cianfarani, S. Uteroplacental insufficiency down regulates insulin receptor and affects expression of key enzymes of long-chain fatty acid (LCFA) metabolism in skeletal muscle at birth. *Cardiovasc. Diabetol.* **2008**, *7*, 14.
- (95) Lane, R. H.; Kelley, D. E.; Ritov, V. H.; Tsirka, A. E.; Gruetzmacher, E. M. Altered expression and function of mitochondrial beta-oxidation enzymes in juvenile intrauterine-growth-retarded rat skeletal muscle. *Pediatr. Res.* **2001**, *50* (1), 83–90.
- (96) Maceyka, M.; Payne, S. G.; Milstien, S.; Spiegel, S. Sphingosine kinase, sphingosine-1-phosphate, and apoptosis. *Biochim. Biophys. Acta, Mol. Cell Biol. Lipids* **2002**, *1585* (2–3), 193–201.
- (97) Spiegel, S.; Milstien, S. Sphingosine 1-phosphate, a key cell signaling molecule. *J. Biol. Chem.* **2002**, *277* (29), 25851–25854.
- (98) Fruhwirth, G. O.; Loidl, A.; Hermetter, A. Oxidized phospholipids: from molecular properties to disease. *Biochim. Biophys. Acta* **2007**, *1772* (7), 718–736.
- (99) Tincani, A.; Cavazzana, I.; Ziglioli, T.; Lojaco, A.; De Angelis, V.; Meroni, P. Complement activation and pregnancy failure. *Clin. Rev. Allergy Immunol.* **2010**, *39* (3), 153–159.
- (100) Bobrow, C. S.; Soothill, P. W. Fetal growth velocity: a cautionary tale. *Lancet* **1999**, *353* (9163), 1460–1460.